COVER PAGE

Document downloaded by @DAEL

Fri May 22 17:01:31 2026

For personal use

When automatic English translation is provided, only the original document is authentic.

The EAA cannot be held responsible of any translation error

Bibliographical reference

The Harmonoise Sound Propagation Model, Erik Salomons, Dirk Van Maercke, Jérôme Defrance and Foort De Roo, Acta Acustica **vol. 97** (Number 1), 2011, pp. 62-74

DOI

https://doi.org/10.3813/AAA.918387

ACTA ACUSTICA UNITED WITH ACUSTICA
Vol. 97 (2011) 62 – 74

DOI 10.3813/AAA.918387

The Harmonoise Sound Propagation Model

Erik Salomons[1)], Dirk van Maercke[2)], Jérôme Defrance[2)], Foort de Roo[3)]

[1)] TNO Built Environment and Geosciences, Van Mourik Broekmanweg 6, 2628 XE Delft, The Netherlands. erik.salomons@tno.nl

[2)] CSTB Grenoble, 24 rue Joseph Fourier, F-38400 Saint Martin d'Hères, France

[3)] TNO Science and Industry, Stieltjesweg 1, 2628 CK Delft, The Netherlands

Summary

The Harmonoise model for predicting environmental noise is expected to provide a basis for the development of a future method for environmental noise mapping in Europe. In this article a detailed description is presented of all steps involved in a calculation with the Harmonoise sound propagation model. The description is restricted to point-to-point propagation, which is a basic element of a full (engineering) model for environmental noise. The description provides all details that are required for developing a computer code for the Harmonoise point-to-point model. The development and the theoretical justification of the model was described by D. van Maercke and J. Defrance in Acta Acustica united with Acustica **93** (2007) 201–212. In the present article some recent improvements of the model are included. Numerical examples are also presented. Results of the Harmonoise model are compared with results of the Nord2000 model, and also with accurate reference results. Also included are reference results that illustrate the effect of linearizing logarithmic wind profiles, which is relevant as Harmonoise and Nord2000 assume linearized wind profiles.

PACS no. 43.28.En, 43.28.Fp, 43.50.Rq, 43.50.Sr

1. Introduction

To regulate and control the harmful effects of environmental noise, the European Commission requires that EU Member States produce noise maps for road traffic noise, rail traffic noise, aircraft noise, and industry noise [1]. The noise maps should be represented by exposure distributions of the inhabitants. The first round of EU noise mapping took place in 2007/2008 and the next round will be in 2012.

A problem with the EU noise maps is that there is not (yet) a standard European model for calculating the sound levels. For the EU noise maps of 2007/2008 various national calculation models have been used, which makes the comparison of noise maps from different Member States rather ambiguous. To solve the problem the European Commission is currently investigating the possibilities to develop a common European model for future noise mapping rounds. Such a model may be based on the models Harmonoise and/or Nord2000. The Harmonoise model was developed in the European projects Harmonoise and Imagine [2]. The Nord2000 model was developed in a Scandinavian project [3, 4].

As a contribution to the above European development, this article presents a description of all steps involved in a calculation with the Harmonoise sound propagation model. The description is restricted to *point-to-point propagation*. The practical problem of representing an extended source (a road for example) by a number of point sources is not addressed here. Also the problem of reflections by vertical surfaces (facades, noise barriers), which may be formulated by means of image sources, is not addressed in detail.

The formulas for the various calculation steps are presented without derivation or justification. Information on the background of the formulas can be found in reference [5]. The description presented here includes modifications of the Harmonoise model applied during the Imagine project and also recent modifications and optimizations of the model that were applied after a series of test calculations. For simplicity we refer to the model as the Harmonoise model. The most important differences compared to the model described in reference [5] are in the transition model (section 2.4.3) and in the calculation of the effect of atmospheric refraction (section 2.5).

The model description presented here provides all details that are required for developing a computer code for the Harmonoise point-to-point model. The completeness of the description was verified by comparing results of two independent computer codes (one developed in Grenoble and one in Delft).

In this article some numerical examples of point-to-point calculations are also presented. Results of the Harmonoise model are compared with results of the Nord2000 model, and also with accurate reference results. Also included are reference results that illustrate the effect of lin-

Received 22 January 2010,
accepted 8 October 2010.

© S. Hirzel Verlag · EAA

Document downloaded by @DAEL, 2026-05-22 17:01:36 - personal use only

earizing logarithmic wind profiles, which is relevant as Harmonoise and Nord2000 assume linearized wind profiles (or more general, sound speed profiles). The numerical examples and comparisons were previously reported in [6], while similar comparisons were reported in [7].

The description of the Harmonoise sound propagation model is presented in section 2 and the numerical examples and comparisons are presented in section 3.

2. Description of the Harmonoise sound propagation model

In section 2.1 the set-up of the Harmonoise model is described, with basic quantities such as source level, propagation attenuation, and excess attenuation. In section 2.2 a recursive calculation scheme for the excess attenuation is described. The excess attenuation consists of diffraction attenuation and ground attenuation, which are calculated with formulas presented in sections 2.3 and 2.4, respectively. Section 2.5 describes how atmospheric refraction is taken into account in the model. Section 2.6 describes the effect of scattering of sound waves by atmospheric turbulence.

2.1. Setup of the Harmonoise model

A situation is considered with a sound source and a receiver. The sound level L at the receiver is written as the sum of a source level L_{source} and a propagation term ΔL_{prop},

$$L = L_{\text{source}} + \Delta L_{\text{prop}}. \tag{1}$$

Strictly speaking the propagation term ΔL_{prop} is equal to *minus* the propagation attenuation, but for simplicity this quantity will be referred to as the propagation attenuation. The propagation attenuation is written as

$$\Delta L_{\text{prop}} = \Delta L_{\text{geo}} + \Delta L_{\text{air}} + \Delta L_{\text{excess}}, \tag{2}$$

with geometrical attenuation ΔL_{geo}, attenuation due to air absorption $\Delta L_{\text{air}} = -\alpha_{\text{air}} r$, excess attenuation ΔL_{excess}, where r is the source-receiver distance and α_{air} is the air absorption coefficient in dB/m, which is calculated with ISO 9613-1 [8]. The geometrical attenuation depends on the type of source; for a point source it is $\Delta L_{\text{geo}} = -10\log_{10}(4\pi r^2)$, but for a line source (segment) a different formula applies.

It follows from equations (1) and (2) that the excess attenuation can be defined as a level difference,

$$\Delta L_{\text{excess}} = L - L_{\text{free}}, \tag{3}$$

where $L_{\text{free}} = L_{\text{source}} + \Delta L_{\text{geo}} + \Delta L_{\text{air}}$ is the sound level at the receiver in free-field conditions (no ground, no obstacles, no wind, and no temperature gradients).

The excess attenuation accounts for complex propagation effects such as atmospheric refraction and turbulence scattering, ground reflection, and screening (diffraction) by obstacles. For the calculation of the excess attenuation it is assumed that the source can be represented by one or more point sources. For example, a line source is first represented by a set of line segments, and next each segment is represented by a point source at the centre of the segment for the calculation of the excess attenuation.

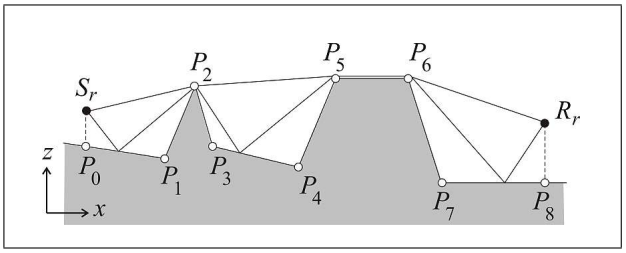

Figure 1. Example of a point-to-point propagation geometry, with source S_r, receiver R_r, and a ground profile with vertices P_i.

The remainder of section 2 describes the calculation of the excess attenuation for sound propagation from a point source to a receiver.

2.2. Excess attenuation

2.2.1. Ground profile and atmospheric refraction

The model assumes a ground profile between the source and the receiver that consists of N straight line segments with end points P_i with $i = 0, 1, \ldots, N$ (see Figure 1). The xz coordinates of the vertices P_i are (x_i, z_i), with the condition $x_{i+1} > x_i$. The ground segments are labelled with index $k = 0, 1, \ldots, N-1$. The first ground segment is $P_0 - P_1$, the second segment is $P_1 - P_2$, etc.

The source S_r is located at position $(x_0, z_0 + H_S)$ and the receiver R_r is located at position $(x_N, z_N + H_R)$, with (local) source and receiver heights H_S and H_R. Subscript r is used to distinguish *real* source S_r and *real* receiver R_r from *general* source S and *general* receiver R, which may be the real source/receiver or a secondary source/receiver at a diffraction edge. The source and receiver heights are subject to statistical uncertainties as described in section 2.4.1.

The effect of atmospheric refraction is taken into account by a curvature of the ground profile (see [9], for example), as described in section 2.5. A coordinate transformation is applied to the ground vertices P_i, while the source and the receiver remain at heights H_S and H_R above the transformed vertices P_0 and P_N, respectively (with height measured along the transformed z-axis).

2.2.2. Diffraction, reflection, and scattering

The excess attenuation in equation (2) is written as

$$\Delta L_{\text{excess}} = 10\log_{10}\left(10^{\Delta L/10} + 10^{\Delta L_{\text{scat}}/10}\right), \tag{4}$$

where ΔL represents sound that reaches the receiver by diffraction and reflection by the ground profile, and ΔL_{scat} represents sound that reaches the receiver by scattering at turbulent fluctuations in the atmosphere.

The term L_{scat} is specified in section 2.6. The term ΔL is described in the remainder of this section and sections 2.3 and 2.4.

Document downloaded by @DAEL, 2026-05-22 17:01:36 - personal use only

2.2.3. Recursive calculation scheme for excess attenuation

The excess attenuation ΔL is determined with a recursive calculation scheme, which is described in this section.

Basically, the calculation scheme divides the ground profile into a number of *ground sections* between *diffraction edges*, and the excess attenuation is calculated as a sum of two types of contributions:

1. diffraction attenuations corresponding to the diffraction edges,
2. ground attenuations corresponding to the ground sections.

For the example shown in Figure 1, the diffraction edges are P_2, P_5, and P_6 and the ground sections are $P_0 - P_2$, $P_2 - P_5$, $P_5 - P_6$, and $P_6 - P_8$.

The calculation consists of three steps.

Step 1) From the ground vertices P_i (x_i, z_i) the set of points $P_{i*}(x_i, z_i + H_i)$ is derived, with $H_0 = H_S$, $H_N = H_R$, and $H_i = 0$ for $i = 1, \ldots, N-1$. This implies: $P_{i*} = \{S_r, P_1, P_2, \ldots, P_{N-1}, R_r\}$ for $i = 0, \ldots, N$.

Step 2) Indices i and j are initialized: $i = 0$ and $j = N$.

Step 3) The excess attenuation $\Delta L = \Delta L(P_i, P_j)$ is calculated.

First the set of points P_k with $i < k < j$ above the line from source point P_{i*} to receiver point P_{j*} is determined.

If the set of points P_k is empty, the result ΔL of step 3 is equal to the ground attenuation $\Delta L_G(P_i, P_j)$. In this case there are no diffraction edges above the line from the source to the receiver.

If the set of points P_k is not empty, then the following two (sub)steps are performed.

i) From the set of points P_k, the point P_k with the largest path length difference

$$\delta(P_{i*}, P_k, P_{j*}) = d(P_{i*}, P_k) + d(P_k, P_{j*}) - d(P_{i*}, P_{j*}) \tag{5}$$

is selected, where $d(P, Q)$ is the distance between points P and Q.

ii) The result ΔL of step 3 is given by

$$\Delta L_D(P_{i*}, P_k, P_{j*}) + \Delta L(P_i, P_k) + \Delta L(P_k, P_j), \tag{6}$$

where the term ΔL_D represents a diffraction attenuation for the sound path P_{i*}–P_k–P_{j*} and the last two terms are determined by repeated application of step 3.

The first time step 3 is performed, P_{i*} and P_{j*} correspond to the *real* source S_r and the *real* receiver R_r, respectively. The next times, however, P_{i*} and/or P_{j*} correspond to a *secondary* source S at a diffraction edge and/or a *secondary* receiver R at a diffraction edge, respectively.

The calculation of the diffraction attenuation ΔL_D is described in section 2.3. The calculation of the ground attenuation ΔL_G is described in section 2.4.

2.2.4. Frequency and wavelength

The excess attenuation, and also the attenuation due to air absorption in equation (2), are functions of the frequency f. With the Harmonoise model, the attenuations are evaluated at *centre frequencies* of frequency bands. The centre frequencies are indicated as f_n, with $n = 1, 2, \ldots$. For example, one may use the 27 one-third octave bands from 25 Hz to 10 kHz ($f_1 = 25$ Hz, $f_{27} = 10$ kHz). The effect of frequency band averaging is considered in section 2.4.1.

The wavelength is given by the relation $\lambda = c_0/f$, with sound speed c_0. The sound speed is a function of the absolute temperature T (in Kelvin): $c_0 = c_{\text{ref}}\sqrt{T/T_{\text{ref}}}$, with $c_{\text{ref}} = 331$ m/s and $T_{\text{ref}} = 273$ K (cf. section 2.5). For $T = 288$ K the sound speed is 340 m/s.

The wavenumber is given by $k = 2\pi f/c_0$.

2.3. Diffraction attenuation

The diffraction attenuation $\Delta L_D(S, P, R)$ is calculated with the following formula due to Deygout [10] for the situation shown in Figure 2:

$$\Delta L_D(N_F) = \begin{cases} 0 & \text{for } N_F < -0.25, \\ -6 + 12\sqrt{-N_F} & \text{for } -0.25 \le N_F < 0, \\ -6 - 12\sqrt{N_F} & \text{for } 0 \le N_F < 0.25, \\ -8 - 8\sqrt{N_F} & \text{for } 0.25 \le N_F < 1, \\ -16 - 10\log N_F & \text{for } N_F \ge 1, \end{cases} \tag{7}$$

with Fresnel number

$$N_F = 2\delta/\lambda. \tag{8}$$

Here δ is a (signed) path length difference between the diffracted path S–P–R and the direct path S–R, as specified below.

Use is made of distances d_S and d_R and diffraction angles θ_S and θ_R, indicated in Figure 2, and angle $\theta = \theta_S + \theta_R$. Diffraction angles θ_S and θ_R are measured with respect to the vertical line at point P, counter clockwise for the source S (or the image source S') and clockwise for the receiver R (or the image receiver R'). Image source S' and image receiver R' are used in section 2.4. Angle θ satisfies $0 < \theta < 4\pi$, if one considers all possible positions of the (image) source and the (image) receiver. Two regions are distinguished: $\theta \le \pi$ and $\theta > \pi$.

For $\theta \le \pi$, parameter δ is given by the usual geometrical definition of the (signed) path length difference,

$$\delta = -\left(d_S + d_R - d_d\right), \tag{9}$$

with direct path length

$$d_d = \sqrt{d_S^2 + d_R^2 - 2d_S d_R \cos\theta}. \tag{10}$$

Parameter δ is negative for $\theta < \pi$, and zero for $\theta = \pi$.

For $\theta > \pi$, an analytical continuation of the geometrical definition of parameter δ is used (which closely agrees

Document downloaded by @DAEL, 2026-05-22 17:01:36 - personal use only

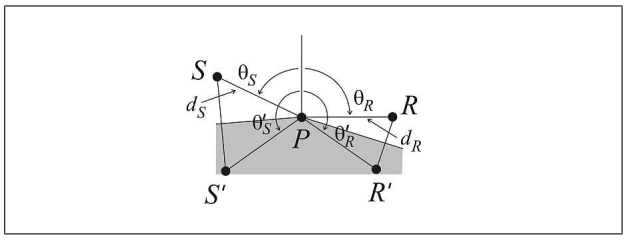

Figure 2. Diffraction geometry with source S, receiver R, and diffraction edge P (the grey area is a part of a ground profile as shown in Figure 1). Indicated are diffraction angles θ_S and θ_R, distance d_S between S and P, and distance d_R between P and R. Also indicated are image source S' and image receiver R'.

with the usual geometrical definition for $\pi < \theta < 1.5\pi$, but remains valid for $\theta > 1.5\pi$):

$$\delta = d_d\left(\frac{1}{2}\varepsilon^2 + \frac{1}{3}\varepsilon^4\right), \tag{11}$$

with

$$d_d = d_S + d_R, \tag{12}$$

$$\varepsilon = \frac{\sqrt{d_S d_R}}{d_S + d_R}\left(\theta - \pi\right). \tag{13}$$

From ΔL_D a (normalized) diffracted sound pressure amplitude p_D is calculated,

$$p_D = \frac{\mathrm{e}^{\mathrm{i}kd_d}}{d_d} 10^{\Delta L_D/20}, \tag{14}$$

where d_d is defined above for $\theta \leq \pi$ and $\theta > \pi$. Amplitude p_D is used for the calculation of the ground attenuation, as described in section 2.4.

2.4. Ground attenuation

2.4.1. Concave ground model

Geometry For each ground segment a local dh coordinate system is used, with the origin at the normal projection of the source on (the extension of) the segment, the d axis along the segment in the receiver direction and the h axis perpendicular to it (see Figure 3). The h coordinates of the source and the receiver are h_S and h_R, respectively (local heights h_S and h_R should be distinguished from global heights H_S and H_R used in section 2.2).

Three types of ground segments are distinguished, depending on the signs of h_S and h_R:

- concave segments, with $h_S > 0$ and $h_R > 0$,
- convex segments, with $h_S < 0$ or $h_R < 0$,
- hull segments, with $h_S = 0$ and $h_R = 0$.

An example of a hull segment is P_5–P_6 in Figure 1.

In general, the ground between two successive diffraction edges may contain concave segments, convex segments, and hull segments.

In this section (section 2.4.1), only situations with concave segments and / or hull segments are considered. In section 2.4.3 situations with convex segments are considered. To distinguish the two types of situations, the ground

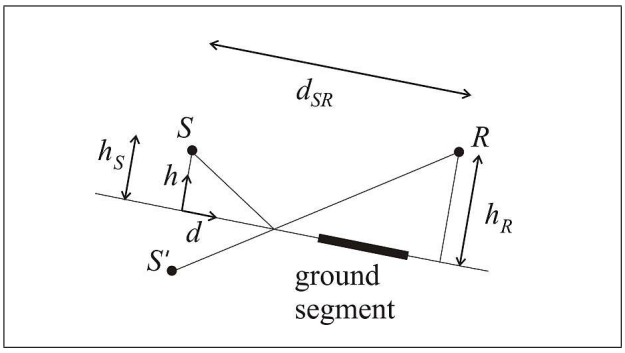

Figure 3. Basic reflection geometry for a ground segment, with source S, image source S', and receiver R. The reflection point is outside the finite ground segment in this example. The local dh coordinate system is also indicated, with dimensions h_S, h_R, and d_{SR}.

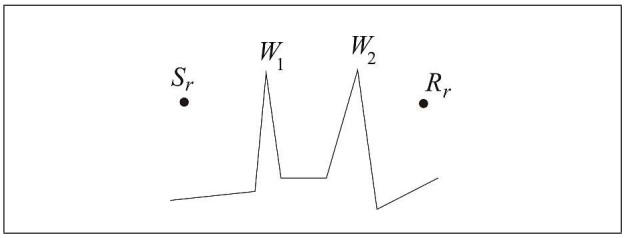

Figure 4. Geometry with two diffraction edges W_1 and W_2 between the source S_r and the receiver R_r.

attenuation ΔL_G is labelled with indices c and t, respectively (c = concave ground model of section 2.4.1, t = transition model of section 2.4.3): ΔL_{Gc} is described in section 2.4.1 and ΔL_{Gt} is described in section 2.4.3.

The formulae below are used to calculate the ground attenuation $\Delta L_{Gc}(P_i, P_j)$ for propagation from a (secondary) source at position $P_{i*}(x_i, z_i + H_i)$ to a (secondary) receiver at position $P_{j*}(x_j, z_j + H_j)$ over ground profile $P_k(x_k, z_k)$ with $k = i, \ldots, j$ (see section 2.2.3).

The distinction between *real* source or receiver and *secondary* source or receiver is illustrated by considering the geometry shown in Figure 4, with two diffraction edges W_1 and W_2. In this case the ground attenuation is calculated for three ground sections:

a) the section between S_r and W_1, with $P_i = S_r$ and $P_j = W_1$,
b) the section between W_1 and W_2, with $P_i = W_1$ and $P_j = W_2$,
c) the section between W_2 and R_r, with $P_i = W_2$ and $P_j = R_r$.

Ground attenuation The ground attenuation ΔL_{Gc} is calculated as a weighted average of two different ground attenuations:

i) ground attenuation $\Delta L_{G,\mathrm{flat}}$ for relatively flat ground,
ii) ground attenuation $\Delta L_{G,\mathrm{valley}}$ for valley-shaped terrain.

The expression given below for flat ground reduces to a well known result for the case of a homogeneous finite-impedance ground. This expression fails for propagation over valley-shaped terrain, and a more realistic expression for this case is given below.

Document downloaded by @DAEL, 2026-05-22 17:01:36 - personal use only

The expression for ΔL_{Gc} is

$$\Delta L_{Gc} = F_G \Delta L_{G,\text{flat}} + (1 - F_G)\Delta L_{G,\text{valley}} \tag{15}$$

with

$$F_G = 1 - \mathrm{e}^{-1/x_G^2}, \tag{16}$$

$$x_G = N_w / \sqrt{1 + (f/f_c)^2}, \tag{17}$$

$$N_w = \sum_{k=i}^{j-1} w_k. \tag{18}$$

Here w_k are modified Fresnel weights of the ground segments and f_c is a transition frequency. These quantities are specified in section 2.4.2.

Ground attenuation $\Delta L_{G,\text{flat}}$ is given:

$$\Delta L_{G,\text{flat}} = \sum_{k=i}^{j-1} w_k \Delta L_{G,\text{flat},k}, \tag{19}$$

with

$$\Delta L_{G,\text{flat},k} = 10 \log_{10} \Big(\big| 1 + C_k D_k Q_k \big|^2 + (1 - C_k^2) \big| D_k Q_k \big|^2 \Big), \tag{20}$$

and ground attenuation $\Delta L_{G,\text{valley}}$ is given by

$$\Delta L_{G,\text{valley}} = 10 \log_{10} \left(\left| 1 + \sum_{k=i}^{j-1} w_k C_k D_k Q_k \right|^2 + \sum_{k=i}^{j-1} w_k (1 - C_k^2) \big| D_k Q_k \big|^2 \right), \tag{21}$$

where

- Q_k is a spherical-wave reflection coefficient (see section 2.4.1),
- D_k is a geometrical weighting factor (see section 2.4.1),
- C_k is a coherence factor (see section 2.4.1),
- w_k is a modified Fresnel weight (see section 2.4.2).

The summations in equations (19) and (21) are over the ground segments $k = i, \ldots, j-1$ between the source and the receiver. The expression for the ground attenuation for flat ground is well known. The expression for valley-shaped terrain is based on work preformed in [3] and [11].

Spherical-wave reflection coefficient The spherical-wave reflection coefficient Q_k must be calculated for the ground segments $k = i, \ldots, j-1$. For simplicity, subscript k is omitted in this section.

The solution of Chien and Soroka [12] for the spherical-wave reflection coefficient has been slightly modified to obtain a solution that is more realistic for grazing propagation.

The modified solution is

$$Q = R_p + (1 - R_p) F_Q^{n_G}, \tag{22}$$

where $R_p = (Z \cos\alpha - 1)/(Z \cos\alpha + 1)$ is the plane-wave reflection coefficient, α is the reflection angle with respect to the normal on the surface, Z is the normalized ground impedance, F_Q is the boundary-loss factor given by Chien and Soroka, (this factor is a complex function of geometrical parameters, the normalized impedance, and the frequency; the function is specified in [12]; see [13] for numerical evaluation of F_Q), and n_G is given by

$$n_G = 1 - 0.7 \exp\big(- h_m / h_G \big), \tag{23}$$

with $h_m = (h_S + h_R)/2$ and $h_G = \lambda/32$. For $n_G = 1$ equation (22) reduces to the solution of Chien and Soroka. It should be noted that the finite size of a ground segment is ignored for the calculation of Q (see Figure 3).

Geometrical weighting factor The geometrical weighting factor D_k accounts for differences in free field and diffracted field between direct sources/receivers and image sources/receivers. For the calculation of the geometrical weighting factor D_k, four cases are distinguished. The four cases include three cases corresponding to the three ground sections (a–c) described before and one case without diffraction.

Case 1. $i = 0$ and $j = N$ (no diffraction).

In this case we have

$$D_k = \frac{p_F(S'_{r,k}, R_r)}{p_F(S_r, R_r)}, \tag{24}$$

with

$$p_F(S_r, R_r) = \frac{\mathrm{e}^{\mathrm{i}kd(S,R)}}{d(S, R)}. \tag{25}$$

Here $S'_{r,k}$ is the image source of source S_r corresponding to ground segment k, indicated in Figure 3.

Case 2. $i = 0$ and $j < N$ (for example, case a described before).

In this case the factor D_k is given by

$$D_k = \frac{p_D(S'_{r,k}, P_j, R_r)}{p_F(S_r, P_j, R_r)}, \tag{26}$$

where p_D is given by equation (14).

Case 3. $i > 0$ and $j = N$ (for example, case c described before).

In this case the factor D_k is given by

$$D_k = \frac{p_D(S_r, P_i, R'_{r,k})}{p_D(S_r, P_i, R_r)}. \tag{27}$$

Here $R'_{r,k}$ is the image receiver of receiver R_r corresponding to ground segment k.

Case 4. $i > 0$ and $j < N$ (for example, case b described before).

In this case the factor D_k is given by

$$D_k = \frac{p_D(S_r, P_i, P'_{j,k})}{p_D(S_r, P_i, P_j)} \frac{p_D(P'_{i,k}, P_j, R_r)}{p_D(P_i, P_j, R_r)}. \tag{28}$$

Here $P'_{i,k}$ and $P'_{j,k}$ are the image vertices of vertices P_i and P_j, respectively, corresponding to ground segment k.

Document downloaded by @DAEL, 2026-05-22 17:01:36 - personal use only

Coherence factor The coherence factor C_k is a real number between zero and one, given by

$$C = C_a C_b, \tag{29}$$

where subscript k has been omitted for simplicity. Factors C_a and C_b account for fluctuations of the phase difference between direct sound and reflected sound.

Factor C_a is given by

$$C_a = \exp\Big(-\frac{1}{2}\sigma_\varphi^2\Big), \tag{30}$$

where σ_φ is the standard deviation of the fluctuation of the phase difference φ, which is calculated with the relation

$$\varphi = k\big[d(S', R) - d(S, R)\big] \approx \frac{2\pi f}{c_0}\frac{2h_S h_R}{D_{SR}}, \tag{31}$$

with $D_{SR} = d(S, R)$. From equation (31) it follows that σ_φ depends on the standard deviations σ_f, σ_{c_0}, $\sigma_{D_{SR}}$, σ_{h_S}, and σ_{h_R} of the quantities f, c_0, D_{SR}, h_S, and h_R, respectively, by the following relation:

$$\Big(\frac{\sigma_\varphi}{\varphi}\Big)^2 = \Big(\frac{\sigma_f}{f}\Big)^2 + \Big(\frac{\sigma_{c_0}}{c_0}\Big)^2 + \Big(\frac{\sigma_\varphi}{\varphi}\Big)^2 + \Big(\frac{\sigma_{D_{SR}}}{D_{SR}}\Big)^2 + \Big(\frac{\sigma_{h_S}}{h_S}\Big)^2 + \Big(\frac{\sigma_{h_R}}{h_R}\Big)^2, \tag{32}$$

where $\varphi = k[d(S', R) - d(S, R)]$ is used in the denominator on the left-hand-side. The first term on the right-hand-side is used to account for frequency band integration (the excess attenuation is calculated only at centre frequencies of one-third octave bands; see section 2.2.4). This term is given by

$$\frac{\sigma_f}{f} = \frac{1}{3}\frac{\Delta f}{f} = \frac{1}{3}\big(2^{B/2} - 2^{-B/2}\big), \tag{33}$$

with $B = 1/3$ in the case of one-third octave bands (and $B = 1$ in the case of octave bands).

In the second term, a default value of zero is used for σ_{c_0} (so this term is neglected, since fluctuations of the sound speed are taken into account separately by coherence factor C_b). In the third term, a default value of zero is used for $\sigma_{D_{SR}}$ (so this term is neglected). In the fourth term and the fifth term, the standard deviations σ_{h_S} and σ_{h_R} are input parameters of the model, which should be specified in combination with the heights h_S and h_R. The fourth term is taken into account only for the case $i = 0$ (in which the source is the *real* source); for the case $i > 0$ (in which the source is a *secondary* source) the fourth term is neglected. Analogously, the fifth term is taken into account only for the case $j = N$, and neglected for $j < N$.

An upper limit of 1 is applied to the fourth term and the fifth term: Fourth term = $\min(1,(\sigma_{h_S}/h_S)^2)$ and fifth term = $\min(1,(\sigma_{h_R}/h_R)^2)$.

Factor C_b in equation (29) is given by

$$C_b = \exp\Big(-\frac{3}{8}D_T\gamma_T k^2 \rho^{5/3} D_{SR}\Big), \tag{34}$$

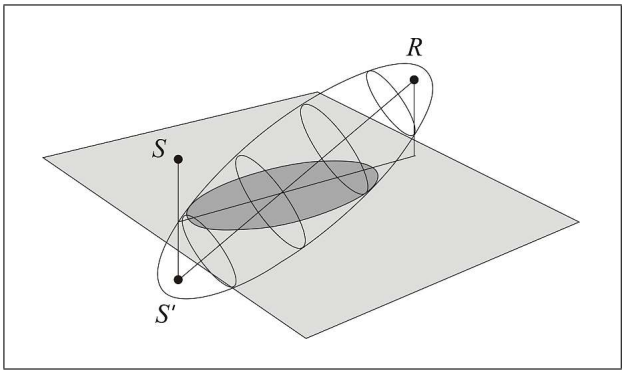

Figure 5. Illustration of the Fresnel ellipsoid for a sound ray from a source S to a receiver R above a reflecting plane (light grey area). The image source S' is also indicated.

with

$$\gamma_T = \Big(\frac{C_T}{T}\Big)^2 + \frac{22}{3}\Big(\frac{C_W}{c_0}\Big)^2, \tag{35}$$

where $D_T = 0.364$ is a constant, C_W and C_T are turbulence structure parameters for wind speed and temperature fluctuations, respectively, and ρ is equal to half the mean separation of the direct and reflected ray paths,

$$\rho = \frac{h_S h_R}{h_S + h_R}. \tag{36}$$

In the case of a hull segment we have $h_S = 0$ and $h_R = 0$, and equation (36) is replaced with $\rho = 0$.

In practice, it is difficult to measure or predict the turbulence structure parameters C_W and C_T. Therefore, γ_T is considered as an input parameter of the model. A typical value of γ_T for 'moderate turbulence' is $5 \cdot 10^{-6}$.

2.4.2. Fresnel weights

This section describes the calculation of the modified Fresnel weights w_k, which were introduced in section 2.4.1. The calculation proceeds in two steps. First 'unmodified' Fresnel weights are calculated as described below. Using the unmodified Fresnel weights, modified Fresnel weights are calculated as described later in this section.

Fresnel weighting The Fresnel ellipsoid for a reflected ray path is a three-dimensional surface that consists of the set of points P satisfying

$$d(S', P) + d(P, R) = d(S', R) + \lambda/n_F, \tag{37}$$

where $d(P, Q)$ is the distance between points P and Q (in three dimensions). The ellipsoid is illustrated in Figure 5. The Fresnel parameter n_F is given by

$$n_F = 8. \tag{38}$$

(For the modified Fresnel weights described later a frequency-dependent Fresnel parameter n_F is used, which is given in equation 59).

The Fresnel ellipse is defined as the intersection of the Fresnel ellipsoid and the reflecting plane (see Figure 6). A

Document downloaded by @DAEL, 2026-05-22 17:01:36 - personal use only

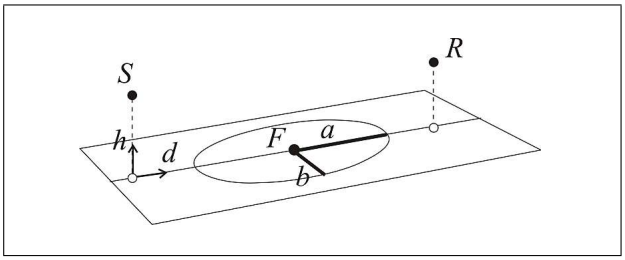

Figure 6. Illustration of the Fresnel ellipse and the local *hd* coordinate system. The ellipse has centre F and axes with lengths $2a$ and $2b$. The centre does not coincide with the point of specular reflection.

local *dh* coordinate system is used, with the origin at the normal projection of the source on the plane (see Figure 6 and Figure 3). The local source coordinates are $(0, h_S)$ and the local receiver coordinates are (d_{SR}, h_R).

The d coordinate of the centre F of the Fresnel ellipse is given by

$$d_F = \frac{d_{SR}}{2}\left(1 + \frac{h_S^2 - h_R^2}{D^2 - d_{SR}^2}\right), \tag{39}$$

and parameter a, i.e. half the long axis of the ellipse (see Figure 6), is given by

$$a = \frac{1}{2}\sqrt{\frac{D^4 + (D_S^2 - D_R^2)^2 - 2D^2(D_S^2 + D_R^2)}{D^2 - d_{SR}^2}}. \tag{40}$$

Here we have introduced the following quantities:

$$D = \lambda/n_F + \sqrt{(h_S + h_R)^2 + d_{SR}^2}, \tag{41}$$

$$D_S^2 = d_F^2 + h_S^2, \tag{42}$$

$$D_R^2 = (d_{SR} - d_F)^2 + h_R^2. \tag{43}$$

In general, a Fresnel weight of a ground region is equal to the area of the region that lies within the Fresnel ellipse divided by the total area of the Fresnel ellipse. Here the calculation is performed in two dimensions, so each ground segment represents a strip that is infinitely long in the third dimension.

The Fresnel weight $w_{F,k}$ of a ground segment k extending from $d = d_1$ to $d = d_2$ is given by

$$w_{F,k} = F_w(\xi_2) - F_w(\xi_1), \tag{44}$$

with function F_w given by

$$F_w(x) = \tag{45}$$
$$\begin{cases} 0 & \text{for } x \le -1, \\ 1 - \frac{1}{\pi}\left(\cos^{-1}(x) - x\sqrt{1-x^2}\right) & \text{for } -1 < x < 1, \\ 1 & \text{for } x \ge 1, \end{cases}$$

and parameter ξ_m given by

$$\xi_m = \frac{d_m - d_F}{a}, \qquad (m = 1, 2). \tag{46}$$

Since the model uses no segments to the left of the source and to the right of the receiver, equation (45) must be modified for the first segment and the last segment:
$F_w = 0$ for the left-end point of the first segment ('foot point' of the source),
$F_w = 1$ for the right-end point of the last segment ('foot point' of the receiver).
This ensures that the relation $\sum w_{F,k} = 1$ is satisfied for a homogeneous infinite flat ground surface, as required.

Equations (45) and (46) imply $F_W = 0.5$ for $\xi = 0$, or $d = d_F$, which means that the Fresnel weighting is centred at the centre of the Fresnel ellipse. It has been found that this approach works fairly well at low frequency, but requires modification at high frequency (see [5]). The modified Fresnel weighting described below is centred at a point that lies between the centre of the Fresnel ellipse and the specular reflection point.

Modified Fresnel weighting It has been found that the Fresnel weights described before work well at low frequencies but yield less accurate results at high frequency. Therefore, modified Fresnel weights w_k are used for the calculation of the ground effect for concave ground, described in section 2.4.1. The modified Fresnel weights w_k are given by a similar expression as the Fresnel weights (44) but with modified arguments ξ'_m,

$$w_k = F_w(\xi'_2) - F_w(\xi'_1), \tag{47}$$

with

$$\xi'_m = \frac{\xi_m - \xi_C}{1 - \xi_m\xi_C}, \qquad (m = 1, 2), \tag{48}$$

$$\xi_C = \frac{d_C - d_F}{a}, \tag{49}$$

$$d_C = \alpha(f)d_F + \big(1 - \alpha(f)\big)d_{SP}, \tag{50}$$

$$d_{SP} = d_{SR}\frac{h_S}{h_S + h_R}, \tag{51}$$

$$\alpha(f) = \left[1 + \left(\frac{f}{f_c}\right)^2\right]^{-1}, \tag{52}$$

$$f_c = \sqrt{f_{\min} f_{\max}}. \tag{53}$$

For hull segments h_S and h_R are zero, and equation (51) is replaced with $d_{SP} = 0.5 d_{SR}$.

The modified Fresnel weighting is centred at the point $d = d_C$, which according to equation (50) lies between the centre of the Fresnel ellipse (point F at $d = d_F$) and the specular reflection point ($d = d_{SP}$), depending on the frequency.

Frequency f_c depends on frequencies $f_{\min}$ and $f_{\max}$, which are defined by (a unique solution is obtained by an approach described at the end of this section)

$$\varphi_{\max}(f_{\min}) = \frac{1}{2}\pi, \tag{54}$$

$$\varphi_{\max}(f_{\max}) = \pi, \tag{55}$$

where $\varphi_{\max}$ is the maximum phase difference between direct and reflected sound,

$$\varphi_{\max}(f) = \max_k\big\{\varphi_k(f)\big\}, \tag{56}$$

Document downloaded by @DAEL, 2026-05-22 17:01:36 - personal use only

with

$$\varphi_k(f) = \arg(Q_k) + k\left[d(S'_k, R) - d(S, R)\right], \quad (57)$$

where $\arg(Q)$ is the phase shift upon reflection (i.e. the imaginary part of the complex reflection coefficient Q). Notation $\max_k$ in equation (56) means that the largest value from the values for all ground segments k between the (secondary) source and the (secondary) receiver is used ($i \le k < j$), where two types of segments are excluded:
i) convex segments,
ii) segments with zero Fresnel weight w_F given by equation (44).

The meaning of equations (54) and (55) is that the phase difference $\varphi_{\max}$ is equal to $\pi/2$ for frequency $f_{\min}$ and equal to π for frequency $f_{\max}$. In the model, however, only centre frequencies of frequency bands (e.g. one-third octave bands) are considered. Therefore, the following calculation scheme is used to determine $f_{\min}$ and $f_{\max}$.

For $f_{\min}$, first the lowest centre frequency f_n with $\varphi_k(f_n) \ge \pi/2$ is determined. Next $f_{\min}$ is calculated by linear interpolation,

$$f_{\min} = f_{n-1} + (f_n - f_{n-1})\frac{\pi/2 - \varphi(f_{n-1})}{\varphi(f_n) - \varphi(f_{n-1})} \quad (58)$$

for $n > 1$. For $n = 1$, $f_{\min} = f_n$ is used.

For $f_{\max}$ the calculation is analogous, with $\pi/2$ replaced with π.

The Fresnel parameter n_F for the modified Fresnel weights is given by

$$n_F = 32\left[1 - \exp(f_c^2/f^2)\right], \quad (59)$$

where f_c is the transition frequency (53).

2.4.3. Transition model

In sections 2.4.1 and 2.4.2 the calculation of the ground attenuation was described for situations *without* convex segments, i.e. situations with only concave segments or hull segments. This section describes the calculation for situations with one or more convex segments.

Convex segments This section describes the calculation of quantities Q_k, D_k, C_k, and w_k for a convex segment with $h_S < 0$ and $h_R > 0$ (see Figure 7). The calculation for a convex segment with $h_S > 0$ and $h_R < 0$ is analogous.

The quantities Q_k, D_k, C_k, and w_k are calculated in the same way as for concave segments, using equations (22)–(59), with two modifications:
i) the source S is replaced with the image source S', so h_S is replaced with $-h_S$,
ii) the geometrical weighting factor D_k as described in section 2.4.1 is multiplied with the factor

$$p_D(S, X, R')/p_D(S, X, R), \quad (60)$$

where X is the specular reflection point indicated in Figure 7, S is the original source position (not yet replaced with S') and p_D is the diffraction amplitude given by equation (14).

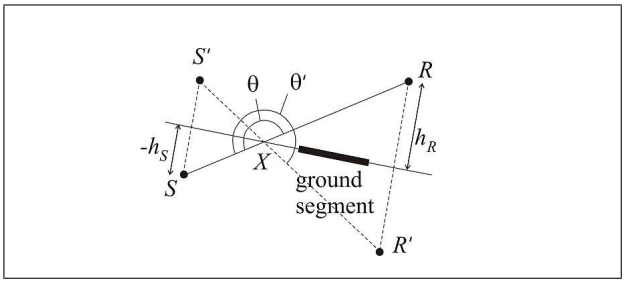

Figure 7. Geometry with convex ground segment, with $h_S < 0$ and $h_R > 0$. For the calculation of the ground effect, the specular reflection point X is used as a diffraction edge.

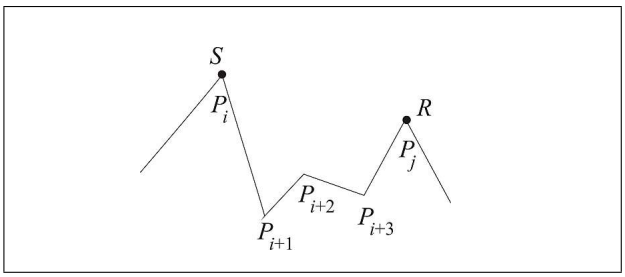

Figure 8. Example of a situation with a convex segment (P_{i+1}–P_{i+2}) between secondary source S and secondary receiver R. Vertex P_{i+2} is used as diffraction edge below the line SR in this case.

For the diffraction amplitude $p_D(S, X, R)$ in equation (60), the diffraction angle θ is equal to π. This implies $p_D(S, X, R) = {}^1\!/_2 p_F(S, R)$ since $\Delta L_D = -6\,\mathrm{dB}$ for $N = 0$ and $\theta = \pi$. For the diffraction amplitude $p_D(S, X, R')$ in equation (60), the diffraction angle θ is larger than π.

Ground attenuation In this section the calculation of the ground attenuation $\Delta L_{Gt}(P_i, P_j)$ introduced in section 2.4.1 is described. This ground attenuation applies to a ground profile P_k ($k = i, \ldots, j$) with at least one convex segment

First one determines the diffraction edge P_k *below* the line SR that has the *smallest* path length difference defined by equation (5). In the search for diffraction edge P_k *only left end-points of convex segments with* $h_S < 0$ and *right end-points of convex segments with* $h_R < 0$ are included. Diffraction edge P_k corresponds roughly to the 'highest peak' below the line SR. Figure 8 shows an example, in which point P_{i+2} is the diffraction edge P_k.

The ground attenuation $\Delta L_{Gt}(P_i, P_j)$ is given by

$$\Delta L_{Gt} = \chi \Delta L_1 + (1 - \chi)\Delta L_2, \quad (61)$$

with
$$\Delta L_1 = \Delta L_D(S, P_k, R) + \Delta L_{Gc}(P_i, P_k) + \Delta L_{Gc}(P_k, P_j), \quad (62)$$
$$\Delta L_2 = \Delta L_{Gc}(P_i, P_j), \quad (63)$$

where ΔL_D is the diffraction attenuation described in section 2.3 and ΔL_{Gc} is the ground attenuation described in

Document downloaded by @DAEL, 2026-05-22 17:01:36 - personal use only

section 2.4.1, taking into account the modified calculation of quantities Q_k, D_k, C_k, and w_k for convex segments as described at the beginning of section 2.4.3.

Factor χ in equation (61) is given by

$$\chi = \chi_2 + (1 - \chi_1)(1 - \chi_2), \tag{64}$$

with factors χ_1 and χ_2 described below. Quantity χ_1 accounts for the 'balance' between reflection and diffraction by the ground segments. Factor χ_2 is included to achieve continuity at the line of sight.

For the calculation of factors χ_1 and χ_2, quantities δ_{dif} and $\delta_{\mathrm{spek},k}$ are used. Quantity δ_{dif} is the path length difference $\delta(S, P_k, R)$ between the diffracted path S–P_k–R and the direct path S–R, as defined by equation (5),

$$\delta_{\mathrm{dif}} = \delta(S, P_k, R). \tag{65}$$

Quantity $\delta_{\mathrm{spek},k}$ is defined as follows, for all ground segments k between S and R:

$$\delta_{\mathrm{spek},k} = d(S'_k, R) - d(S, R), \tag{66}$$

where S'_k is the image source corresponding to ground segment k. For concave segments, $\delta_{\mathrm{spek},k}$ is the path length difference of reflected path S–X_k–R and the direct path S–R, where X_k is the specular reflection point for ground segment k (which may be outside the finite ground segment k). For convex segments, $\delta_{\mathrm{spek},k}$ is negative (the replacement $h_S \to -h_S$ or $h_R \to -h_R$ is *not* used for the calculation of $\delta_{\mathrm{spek},k}$). Quantity $\delta_{\mathrm{spek,avg}}$ is defined as

$$\delta_{\mathrm{spek,avg}} = \frac{\sum_{k=i}^{j-1} w_k \delta_{\mathrm{spek},k}}{\sum_{k=i}^{j-1} w_k}. \tag{67}$$

Quantity χ_1 is given by

$$\chi_1 = \begin{cases} 1 - \exp\left(-1/\tau_1^2\right) & \text{for } \tau_1 > 0, \\ 1 & \text{for } \tau_1 \le 0, \end{cases} \tag{68}$$

with

$$\tau_1 = \frac{\delta_{\mathrm{spek,avg}} - \delta_{\mathrm{dif}}}{\lambda/8}. \tag{69}$$

Quantity χ_2 is given by

$$\chi_2 = \begin{cases} 1 - \exp\left(-1/\tau_2^2\right) & \text{for } \tau_2 > 0, \\ 1 & \text{for } \tau_2 \le 0, \end{cases} \tag{70}$$

with

$$\tau_2 = \frac{\delta_{\mathrm{dif}}}{\lambda/64}. \tag{71}$$

2.5. Atmospheric refraction

As indicated in section 2.2.1, the effect of atmospheric refraction is taken into account by applying a coordinate transformation to the ground vertices P_i, while the source and the receiver remain at heights H_S and H_R vertically above the transformed vertices P_0 and P_N, respectively (with height measured along the transformed z-axis).

Before the coordinate transformation is applied, the segmentation of the ground should be refined in some cases. The maximum segment length $d_{\mathrm{seg,max}}$ is 50 m for source-receiver distances D_{SR} between 150 m and 1 km, $D_{SR}/20$ for distances larger than 1 km, and $D_{SR}/3$ for distances smaller than 150 m. Segments with length d_{seg} larger than $d_{\mathrm{seg,max}}$ are divided into smaller segments of length d_{seg}/M, where M is the smallest integer such that d_{seg}/M is smaller than or equal to $d_{\mathrm{seg,max}}$.

For the effect of atmospheric refraction, a linear vertical profile of the effective sound speed is assumed:

$$c(z) = c_0 \left(1 + \frac{z}{R_c}\right), \tag{72}$$

where c_0 is the sound speed introduced in section 2.2.4 and R_c is a constant. This profile corresponds to circular ray paths with a radius of curvature approximately equal to $|R_c|$. Height z in equation (72) corresponds to the vertical z coordinate indicated in Figure 1.

To take into account the effect of atmospheric refraction (in an indirect way), a coordinate transformation is applied to the system such that circular ray paths transform into straight lines. The calculation scheme described in the previous sections (which was based on straight ray paths) is applied to the transformed system.

The coordinate transformation is the following conformal mapping in the complex plane:

$$w = x + \mathrm{i}z \quad \to \quad w' = x' + \mathrm{i}z', \tag{73}$$

$$w' = \frac{C(w - w_0)}{C + (w - w_0)}, \tag{74}$$

with

$$w_0 = \frac{x_0 + x_N}{2} + \mathrm{i}\frac{z_0 + H_S + z_N + H_R}{2}, \tag{75}$$

$$C = \mathrm{i}C_0, \tag{76}$$

$$C_0 = 2\left(\frac{H_S + H_R}{2} + R_c\right). \tag{77}$$

Here $(x_0, z_0 + H_S)$ and $(x_N, z_N + H_R)$ are the (x, z) coordinates of the source and the receiver, respectively (see section 2.2.1). If this conformal mapping is applied to the two-dimensional wave equation with non-constant sound speed $c(z)$, a transformed wave equation in the $x'z'$ plane is obtained with a sound speed that is constant in good approximation for source-receiver distances $d(S, R)$ up to about $0.2|R_c|$. This implies that the sound speed gradient $c_0/|R_c|$ should not exceed $0.2c_0/d(S, R)$, which yields $0.23\ \mathrm{s}^{-1}$ for $d(S, R) = 300$ m. This limitation is satisfied in the cases considered in section 3. The condition $d(S, R) < 0.2|R_c|$ can also be written as $|R_c| > 5d(S, R)$. So the model should only be applied to cases in which $|R_c|$ is larger than five times the source-receiver distance.

Equations (73) to (77) give

$$x' = \frac{C_0^2 x''}{x''^2 + (C_0 + z'')^2}, \tag{78}$$

$$z' = \frac{C_0(x''^2 + z''^2 + z''C_0)}{x''^2 + (C_0 + z'')^2}, \tag{79}$$

Document downloaded by @DAEL, 2026-05-22 17:01:36 - personal use only

Table I. Specification for 16 cases of the ground flow resistivity in kPa s/m^2 (hard = ∞) and the atmospheric wind profile (zero: non-refracting atmosphere, lin: $a = 0.2\,\mathrm{s}^{-1}$, lin/log: $a = 0.177\,\mathrm{s}^{-1}$, $b = 1$ m/s).

case	ground	wind
1	hard	zero
2	100	zero
3	hard	lin
4	100	lin
5	20000	zero
6	20	zero
7	200	zero
8	200	zero
9	100	lin/log
10	100	zero
11	hard	lin/log
12	hard	zero
13	100	lin/log
14	100	zero
15	hard	lin/log
16	hard	zero

with

$$x'' = x - \frac{x_0 + x_N}{2}, \tag{80}$$

$$z'' = z - \frac{z_0 + H_S + z_N + H_R}{2}. \tag{81}$$

Finally, x' is redefined as x and z' is redefined as z, and the calculation scheme described in the previous sections is applied.

2.6. Scattering by atmospheric turbulence

The effect of scattering of sound waves by atmospheric turbulence is accounted for by adding a scattering term to the excess attenuation, as indicated in equation (4). The scattering term is given by

$$\Delta L_{\mathrm{scat}} = 25 + 10\log_{10}\gamma_T + 3\log_{10}\frac{f}{1000} + 10\log_{10}\frac{D_{SR,\mathrm{hor}}}{100}, \tag{82}$$

where parameter T was introduced in section 2.4.1 and $D_{SR,\mathrm{hor}}$ is the horizontal distance between the (real) source and the (real) receiver. Due to the last term in equation (82), the scattering term increases with increasing distance $D_{SR,\mathrm{hor}}$.

3. Numerical examples

In this section numerical examples are presented for point-to-point propagation, partly based on previous reports [6, 7]. Results of the Harmonoise model are compared with results of the Nord2000 model [3] and accurate reference results.

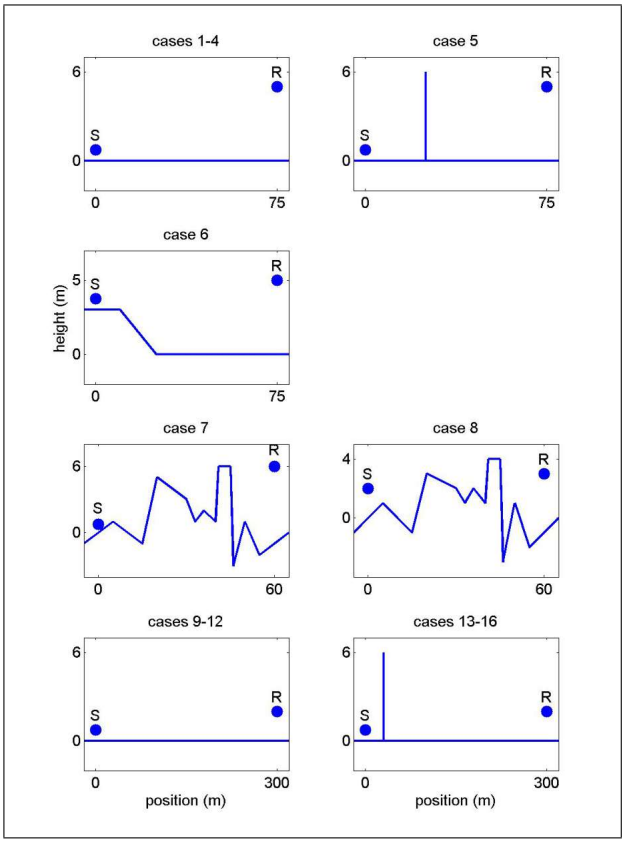

Figure 9. Geometries of 16 cases (S = source, R = receiver).

Calculations were performed for the 16 cases specified in Table I. The calculation geometries are shown in Figure 9. Figure 10 and Figure 11 show the results of the calculations, in terms of 1/3-octave band spectra of the excess attenuation. Parameters of the calculations are specified below for each case.

In all cases, the effect of frequency band averaging through the coherence factor C was included, while other effects of coherence loss were not included. In the reference calculations, averaging over 4 frequencies per 1/3-octave band was performed. For the sound speed c_0 a value of 340 m/s was assumed, corresponding to a temperature of 288 K. The effect of scattering by atmospheric turbulence was ignored. For atmospheric refraction, various wind profiles were assumed, while temperature gradients were ignored. Consequently, the sound speed profile is equal to the sum of sound speed c_0 and the wind speed profile.

In case 1 we have the following parameters: source-receiver distance 75 m, source height 0.75 m, and receiver height 5 m. A hard (rigid) ground and a non-refracting atmosphere (no wind) were assumed. Figure 10 shows that results of Harmonoise (HAR) and Nord2000 (N2K) agree with a reference solution (REF), which in this case is an analytical solution [9] for a point source above a hard ground surface.

Case 2 is similar to case 1, except for the ground: an absorbing ground with a flow resistivity of 100 kPa s/m^2 was assumed. The ground impedance was calculated from

Document downloaded by @DAEL, 2026-05-22 17:01:36 - personal use only

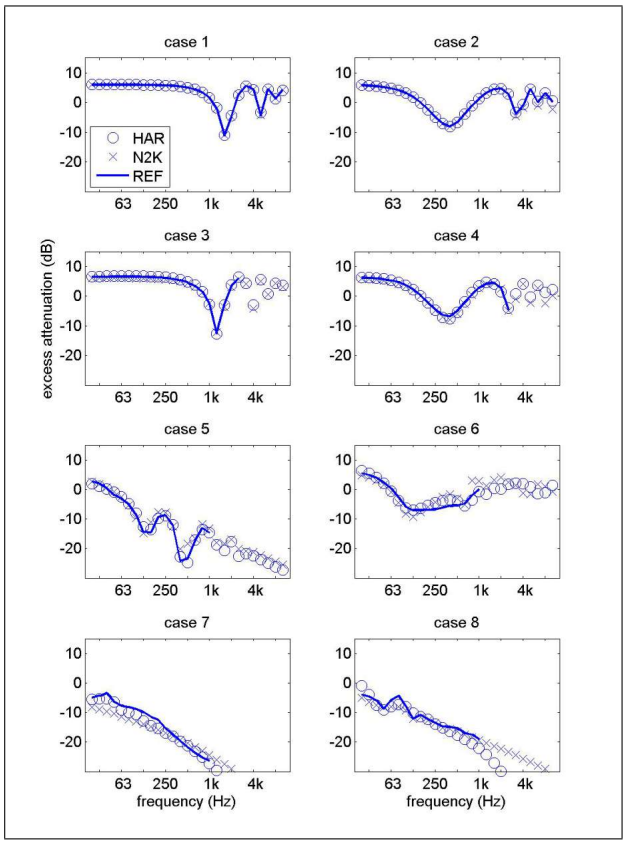

Figure 10. Results for cases 1–8 (HAR = Harmonoise, N2K = Nord2000, and REF = reference solution).

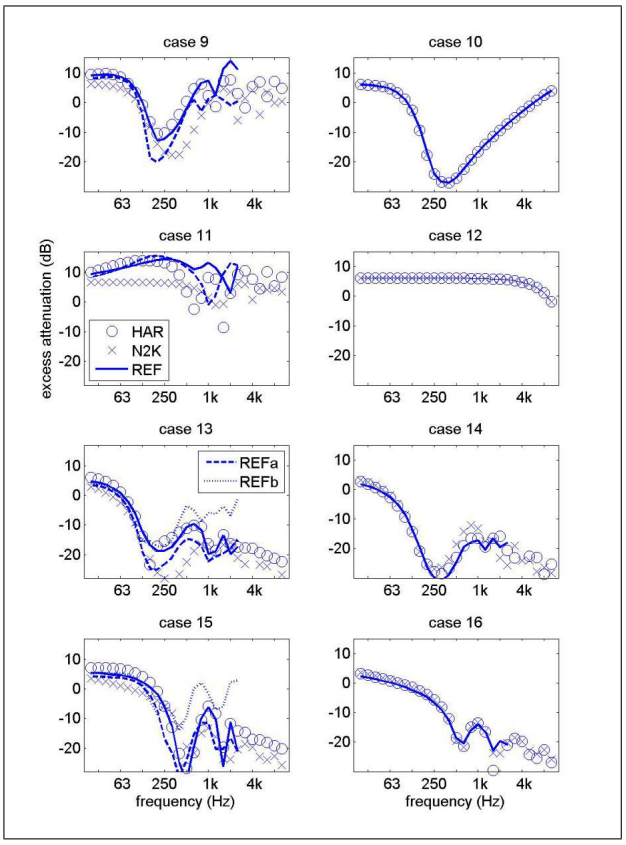

Figure 11. Results for cases 9–16 (REFa = PE for logarithmic profile, REFb = PE for range-dependent profile). Symbols and lines are defined by the legends in the graphs for the cases 11 and 13.

the flow resistivity with the Delany and Bazley model [14] for a semi-infinite porous medium (in all cases). The reference solution is an analytical solution [9] for a point source above an impedance surface. There is good agreement between the three solutions.

Case 3 is similar to case 1, except for the atmosphere: a linear sound speed profile $c = c_0 + az$ was assumed, with $a = 0.2\,\mathrm{s}^{-1}$. The ground interference minimum at 1600 Hz in case 1 is shifted to 1250 Hz in case 3. There is good agreement between the three solutions. The reference solution was calculated with a Greens Function Parabolic Equation (PE) model [9], and was restricted to frequencies up to 2500 Hz for reasons of computational time and memory.

Case 4 is similar to case 2, but again a linear sound speed profile was assumed. There is good agreement between the three solutions.

Case 5 is similar to case 1, but now a 6 m high barrier has been included at 30 m from the source, and an absorbing ground with flow resistivity 20000 kPa s/m^2 was assumed. The reference solution was calculated with a Boundary Element Method, and was restricted to frequencies up to 1000 Hz for reasons of computational time and memory. There is good agreement between the three solutions.

In case 6 we have the following parameters: source-receiver distance 75 m, source height 0.75 m with respect to a 3 m high berm, and receiver height 5 m. A highly absorbing ground was assumed, with flow resistivity 20 kPa s/m^2. The reference solution was calculated with a Boundary Element Method. Deviations from the reference solution are slightly larger for Nord2000 than for Harmonoise, at mid and high frequencies.

In case 7 the source-receiver distance is 60 m, while the ground has an irregular profile and a flow resistivity of 200 kPa s/m^2. The reference solution was calculated with a Boundary Element Method. At low frequency Nord2000 deviates a few decibels from the reference solution.

Case 8 is similar to case 7, but with a slightly modified geometry. Harmonoise and Nord2000 deviate from the reference solution above 1 kHz, but here the excess attenuation is lower than −20 dB, and in this range deviations are usually irrelevant in practice due to sound paths not included here. At low frequency smaller deviations occur.

For cases 9, 11, 13, and 15 (described below), results are presented that illustrate the effect of linearizing the sound speed profile. The linear profile may be considered as an approximation of the (more realistic) logarithmic profile $c = c_0 + b\ln(1 + z/z_0)$, with parameters b and $z_0 = 0.1$ m. For the calculations presented in this article a value of 1 m/s was used for parameter b.

In the Harmonoise and Imagine projects a method was developed to calculate the gradient $a \equiv c_0/R_c$ of the linear profile (see equation 72), in such a way that one may expect results (excess attenuations) that agree as much

Document downloaded by @DAEL, 2026-05-22 17:01:36 - personal use only

as possible for the logarithmic and the linear profile. The scheme was based on the condition that the circular sound ray (sound rays are circle segments for a linear profile) should pass through the source and receiver positions and through the highest point of the sound ray for the logarithmic profile. The resulting formula for the gradient a of the linearized profile is

$$a = c_0\left(\sqrt{B^2 - AC} - B\right)/C,$$

with $A = 1 + \tan^2\theta - \gamma^2$, $B = h_M(1 + \tan^2\theta)$, and $C = h_M^2(1 + \tan^2\theta) + (d/2)^2$ (the formula is valid for $b > 0$). Here the following quantities are used: $\tan\theta = (h_R - h_S)/d_{SR}$, $h_M = (h_S + h_R)/2$, $d = \sqrt{d_{SR}^2 + (h_S - h_R)^2}$, $k = \sqrt{b/(2\pi c_0)}$, and $\gamma = (1+4k^2)/(1-4k^2)$, where h_S is the source height, h_R is the receiver height, and d_{SR} is the horizontal distance between the source and the receiver. Substitution of the values of the parameters for cases 9, 11, 13, and 15 yields $a = 0.177\,\mathrm{s}^{-1}$.

In case 9 we have the following parameters: source-receiver distance 300 m, source height 0.75 m, and receiver height 2 m. An absorbing ground was assumed. Two PE reference solutions are included, one for a logarithmic sound speed profile with $b = 1$ m/s (REFa), and one for the linearized profile with gradient $a = 0.177\,\mathrm{s}^{-1}$ (REF) that was also used for the Harmonoise and Nord2000 solutions. For the linear profile, Harmonoise agrees slightly better with the reference solution than Nord2000 does, but the high excess attenuation of 15 dB at 2 kHz is not reproduced by Harmonoise and Nord2000. For the logarithmic profile (REFa), however, excess attenuations are considerably lower (5–15 dB for 500–2000 Hz). Consequently, Harmonoise and Nord2000 agree slightly better with REFa than with REF, but deviations are still up to 10 dB.

Case 10 is similar to case 9, but now a non-refracting atmosphere is assumed. In this case there is perfect agreement between the three solutions. The reference solution is an analytical solution [9] for a point source above a ground surface (also in cases 12, 14, and 16). We verified that the PE method yields accurate agreement with the analytical solution.

Case 11 is also similar to case 9, but now a hard (rigid) ground is assumed. Again two PE reference solutions are included: one for the logarithmic profile (REFa) and one for the linearized profile (REF). The solutions REF and REFa show excess attenuations above 10 dB for a much wider frequency range than for case 9. The Harmonoise solution agrees better with the reference solutions REF and REFa than Nord2000 does, although there are considerable deviations at high frequency. It is surprising that Harmonoise follows the reference solutions so well until 500 Hz, as the high excess attenuation levels are partly due to multiple ground reflections (see Figure 12), which are not taken into account (explicitly) with the Harmonoise model.

Case 12 is similar to case 11, but now a non-refracting atmosphere is assumed. In this case there is perfect agreement between the three solutions.

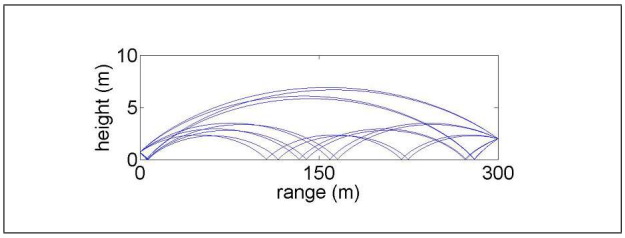

Figure 12. Sound rays for cases 9 and 11 with a logarithmic sound speed profile with $b = 1$ m/s.

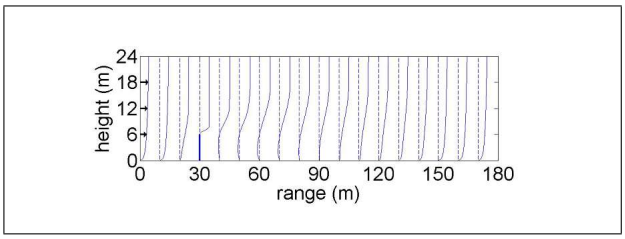

Figure 13. Range-dependent windspeed profile near a 6 m high barrier at range 30 m (thick line), for a logarithmic inflow profile $b\ln(1 + z/z_0)$, with $z_0 = 0.1$ m and $b = 1$ m/s. The horizontal deviation from the vertical dashed lines represents the windspeed. The recirculation region extends to 20 times the barrier height, so to range 150 m.

Case 13 is similar to case 9, but now a 6 m high barrier has been included at 30 m from the source. In addition to the reference solutions for the logarithmic profile (REFa) and for the linearized profile (REF), we have included a reference solution (REFb) for a realistic range-dependent profile taking into account the effect of the barrier on the wind speed profile (see Figure 13) [9, 15]. Solution REFb yields considerably higher levels than the other solutions do, owing to large wind speed gradients near the barrier top (see Figure 13), which are ignored by the other solutions.

Case 14 is similar to case 13, but now a non-refracting atmosphere is assumed. In this case there is fair agreement between the three solutions, although deviations from the reference solution are a bit larger for Nord2000 than for Harmonoise.

Case 15 is similar to case 13, but now a hard (rigid) ground is assumed. Again, the reference solution (REFb) for the realistic range-dependent wind speed profile yields considerably higher levels than the other solutions do. In addition, Harmonoise and Nord2000 deviate from the reference solutions for frequencies below 250 Hz.

Case 16 is similar to case 15, but now a non-refracting atmosphere is assumed. In this case there is good agreement between the three solutions.

4. Concluding remarks

The Harmonoise propagation model is an accurate engineering model for outdoor sound propagation, and represents a 'step forward' with respect to older engineering models such as the ISO model [16]. Harmonoise is applied

Document downloaded by @DAEL, 2026-05-22 17:01:36 - personal use only

to arbitrary terrain profiles with a Fresnel weighting approach that was initially based on the Nord2000 approach and was further developed and fine-tuned by comparison with reference solutions.

Harmonoise differs from Nord2000 by the way in which atmospheric refraction is taken into account. While Nord2000 employs curved sound rays, Harmonoise accounts for refraction by ground curvature. The ground curvature approach seems to work well, at least for small and moderate propagation distances. For large distances, however, multiple ground reflections become important (in particular for hard ground), and these reflections are not taken into account (explicitly) by Harmonoise. In contrast, Nord2000 includes a correction term to account for multiple ground reflections in a downward refracting atmosphere. However, it was found in this study that Harmonoise performs better than Nord2000 for a case with downward refraction over 300 m flat ground, both for hard ground and for absorbing ground.

Both Harmonoise and Nord2000 are restricted to linear sound speed profiles. In this study we have investigated the effect of linearizing the sound speed profile. For propagation over 300 m we found considerable differences between reference solutions for a logarithmic profile and the corresponding linearized profile. Further, we have investigated the influence of the indirect effect of a barrier on sound propagation through the barrier-induced modification of the wind speed profile (a barrier 'blocks' wind). We found that this effect is not predicted accurately by the engineering models Harmonoise and Nord2000. This implies that the small differences between Harmonoise / Nord2000 and reference solutions reported in [4] (the standard deviations was 2.5 dB for Harmonoise and 3.0 dB for Nord2000) may be too optimistic in some cases.

From the 16 cases studied here we conclude that Harmonoise is slightly more accurate than Nord2000 is. This was also concluded in [4], except at very low frequency. Finally, we mention that the application of a point-to-point model such as Harmonoise or Nord2000 to full calculations for complex situations in an urban environment is not straightforward. A problem in an urban environment is that we have to deal with multiple reflections by buildings. In principle this problem can be solved by introducing image sources and image receivers, and using Fresnel weighting to account for the reduction of reflection efficiency with increasing order of reflection (due to the finite ratio of building height over wavelength) [17]. A challenge is to implement these ideas while keeping the model practical and efficient.

Acknowledgement

Valuable help by Birger Plovsing, Gunnar Birnir Jónsson, and Ando Randrianoelina is gratefully acknowledged.

References

[1] European Directive on Environmental Noise, 2002/49/EC. url: http://ec.europa.eu/environment/noise/home.htm, (website of the European Commission).

[2] H. G. Jonasson, M. Dittrich, D. van Maercke, J. Defrance, E. Salomons, I. Noordhoek, D. Heimann, B. Plovsing, G. Watts, X. Zhang, E. Premat, I. Schmich, F. Aballea, M. Baulac, F. de Roo, M. Bakermans, D. Kühner, B. D. Coensel, D. Botteldooren, F. Vanhove, S. Logghe, R. Bütikofer: Building Europe's future harmonized noise mapping methods. Acta Acustica united with Acustica **93** (2007) 173–262. (special issue about the European projects Harmonoise and Imagine). See also URL: http://www.imagine-project.org.

[3] J. Kragh, B. Plovsing, S. A. Storeheier, G. Taraldsen, H. G. Jonasson: Nordic environmental noise prediction method. Nord2000 summary report. General Nordic sound propagation model and applications in source-related prediction methods. DELTA Acoustics and Vibration Report, 1719/01, 2002. Available from www.delta.dk/nord2000, For the numerical examples presented in section 3, a software implementation developed by DELTA Noise & Vibration (Denmark) was used.

[4] G. B. Jónsson, F. Jacobsen: A comparison of two engineering models for outdoor sound propagation: Harmonoise and Nord2000. Acta Acustica united with Acustica **94** (2008) 282–289.

[5] D. van Maercke, J. Defrance: Development of an analytical model for outdoor sound propagation within the Harmonoise project. Acta Acustica united with Acustica **93** (2007) 201–212.

[6] D. van Maercke, E. Salomons: The Harmonoise sound propagation model: further developments and comparison with other models. Proceedings NAG-DAGA conference, Rotterdam, The Netherlands, March 2009.

[7] E. Salomons, D. van Maercke, A. Randrianoelina: Noise barriers and the Harmonoise sound propagation model. Proceedings Euronoise conference, Edinburgh, Scotland, October 2009.

[8] ISO 9613-1:1993(E): Acoustics. Attenuation of sound during propagation outdoors. Part 1: Calculation of the absorption of sound by the atmosphere. International Organization for Standardization, Geneva, Switzerland, 1993.

[9] E. Salomons: Computational atmospheric acoustics. Kluwer, Dordrecht, 2001.

[10] J. Deygout: Multiple knife-edge diffraction by microwaves. IEEE Trans. Antennas and Propagation **14** (1966) 480–489.

[11] D. C. Hothersall, J. N. B. Harriot: Approximate models for sound propagation over multi-impedance plane boundaries. J. Acoust. Soc. Am. **97** (1995) 918–926.

[12] C. F. Chien, W. W. Soroka: A note on the calculation of sound propagation along an impedance surface. J. Sound Vib. **69** (1980) 340–343.

[13] N. Shu, L. F. Cohn, R. A. Harris, T. K. Kim, W. Li: Comparative evaluation of the ground reflection algorithm in FHWA traffic noise model (TNM 2.5). Appl. Acoust. **68** (2007) 1459–1467.

[14] M. E. Delany, E. N. Bazley: Acoustical properties of fibrous absorbent materials. Appl. Acoust. **3** (1970) 105–116.

[15] E. Salomons: Reduction of the performance of a noise screen due to screen-induced wind-speed gradients. Numerical computations and wind-tunnel experiments. J. Acoust. Soc. Am. **105** (1999) 2287–2293.

[16] ISO 9613-2: Acoustics. Attenuation of sound during propagation outdoors. Part 2: General method of calculation. International Organization for Standardization, Geneva, Switzerland, 1996.

[17] J. Forssén, M. Hornikx: Statistics of A-weighted road traffic noise levels in shielded urban areas. Acta Acustica united with Acustica **92** (2006) 998–1008.

Document downloaded by @DAEL, 2026-05-22 17:01:36 - personal use only